ESC European Society of Cardiology

Cardiovascular Research (2019) **115**, 1646–1658
doi:10.1093/cvr/cvz037

Cardiac sodium-dependent glucose cotransporter 1 is a novel mediator of ischaemia/reperfusion injury

Zhao Li[1†], Vineet Agrawal[2‡], Mohun Ramratnam[2,3], Ravi K. Sharma[2], Stephen D'Auria[2], Abigail Sincoular[1], Margurite Jakubiak[1], Meredith L. Music[1], William J. Kutschke[1], Xueyin N. Huang[2], Lindsey Gifford[1], and Ferhaan Ahmad[1,2,4,5]*

[1]Division of Cardiovascular Medicine, Department of Internal Medicine, Carver College of Medicine and Abboud Cardiovascular Research Center, University of Iowa, 100 Newton Road, 1191D ML, Iowa City, IA 52242, USA; [2]Division of Cardiology, Department of Medicine, UPMC Heart and Vascular Institute, University of Pittsburgh, Pittsburgh, PA, USA; [3]Cardiology Section, Medical Service, Division of Cardiovascular Medicine, Department of Medicine, University of Wisconsin, William. S. Middleton Memorial Veterans Hospital, Madison, WI, USA; [4]Department of Radiology, Carver College of Medicine, University of Iowa, Iowa City, IA, USA; and [5]Department of Molecular Physiology and Biophysics, Carver College of Medicine, University of Iowa, Iowa City, IA, USA

Received 8 May 2018; revised 11 December 2018; editorial decision 1 February 2019; accepted 1 February 2019; online publish-ahead-of-print 4 February 2019

Time for primary review: 20 days

Aims We previously reported that sodium-dependent glucose cotransporter 1 (SGLT1) is highly expressed in cardiomyocytes and is further up-regulated in ischaemia. This study aimed to determine the mechanisms by which SGLT1 contributes to ischaemia/reperfusion (I/R) injury.

Methods and results Mice with cardiomyocyte-specific knockdown of SGLT1 ($TG^{SGLT1\text{-}DOWN}$) and wild-type controls were studied. *In vivo*, the left anterior descending coronary artery was ligated for 30 min and reperfused for 48 h. *Ex vivo*, isolated perfused hearts were exposed to 20 min no-flow and up to 2 h reperfusion. *In vitro*, HL-1 cells and isolated adult murine ventricular cardiomyocytes were exposed to 1 h hypoxia and 24 h reoxygenation (H/R). We found that $TG^{SGLT1\text{-}DOWN}$ hearts were protected from I/R injury *in vivo* and *ex vivo*, with decreased infarct size, necrosis, dysfunction, and oxidative stress. 5'-AMP-activated protein kinase (AMPK) activation increased SGLT1 expression, which was abolished by extracellular signal-related kinase (ERK) inhibition. Co-immunoprecipitation studies showed that ERK, but not AMPK, interacts directly with SGLT1. AMPK activation increased binding of the hepatocyte nuclear factor 1 and specificity protein 1 transcription factors to the SGLT1 gene, and HuR to SGLT1 mRNA. In cells, up-regulation of SGLT1 during H/R was abrogated by AMPK inhibition. Co-immunoprecipitation studies showed that SGLT1 interacts with epidermal growth factor receptor (EGFR), and EGFR interacts with protein kinase C (PKC). SGLT1 overexpression activated PKC and NADPH oxidase 2 (Nox2), which was attenuated by PKC inhibition, EGFR inhibition, and/or disruption of the interaction between EGFR and SGLT1.

Conclusion During ischaemia, AMPK up-regulates SGLT1 through ERK, and SGLT1 interacts with EGFR, which in turn increases PKC and Nox2 activity and oxidative stress. SGLT1 may represent a novel therapeutic target for mitigating I/R injury.

Keywords Cardiac ischaemia/reperfusion • SGLT1 • PKC • Nox2 • Reactive oxygen species

1. Introduction

There are two families of cellular glucose transporters, the facilitative glucose transporters (GLUTs) and the sodium-dependent glucose cotransporters (SGLTs).[1] The SGLT1 isoform, encoded by the *SLC5A1* gene, transports glucose by a secondary active transport mechanism that uses the Na^+ gradient established by the Na^+/K^+ ATPase pump. SGLT1 mediates glucose uptake in small intestinal enterocytes and renal

* Corresponding author. Tel: +1 319 384 8756; fax: +1 319 353 6343, E-mail: ferhaan-ahmad@uiowa.edu

† Present address. Department of Pharmaceutical Sciences, University of St. Joseph, West Hartford, CT, USA

‡ Present address. Division of Cardiovascular Medicine, Department of Internal Medicine, Vanderbilt University Medical Center, Nashville, TN, USA

proximal tubule S3 cells.[2] Although SGLT1 mRNA was previously found to be highly expressed in the heart,[3] its cardiac function was never investigated. We recently established that SGLT1 protein is expressed in cardiomyocytes, largely localized to the sarcolemma, and its expression is perturbed in diseases such as ischaemic heart failure, diabetic cardiomyopathy, and glycogen storage cardiomyopathy secondary to mutations in *PRKAG2*.[4,5]

5'-AMP-activated protein kinase (AMPK) is a heterotrimeric enzyme that maintains cellular fuel supply by regulating energy-generating and energy-consuming pathways in response to metabolic needs.[6] AMPK is activated during cardiac ischaemia to restore cardiomyocyte ATP levels by increasing glucose uptake, glycolysis, and free fatty acid oxidation. AMPK activation is associated with protein kinase C (PKC)-dependent up-regulation of GLUT4 expression[7] and translocation of GLUT4 to the sarcolemma, promoting glucose uptake.[8,9] We discovered the first human mutation in the *PRKAG2* gene, encoding the cardiomyocyte-specific γ2 regulatory subunit of AMPK,[10] and other mutations were subsequently identified. We showed that these mutations caused a glycogen storage cardiomyopathy.[11–14] Transgenic mice with these mutations exhibited inappropriate activation of AMPK and elevated cardiac uptake of glucose that was directed to increased glycogen synthesis, leading to the human cardiomyopathy phenotype.[12–15] We discovered that SGLT1 is up-regulated and at least partially mediates the increased cardiac glucose uptake, and that pharmacological[5] and genetic[16] inhibition of SGLT1 attenuates the cardiomyopathy phenotype.

Because of the role of AMPK in the cardiac response to ischaemia and our observation that SGLT1 expression is increased in ischaemia and in *PRKAG2* cardiomyopathy,[4,5] both of which are states characterized by AMPK activation, we sought to determine the mechanism by which SGLT1 is up-regulated in cardiac ischaemia and its potential role in the pathophysiology of ischaemic injury. In this study, we first established that cardiomyocyte-specific knockdown of SGLT1 attenuates injury following regional ischaemia/reperfusion (I/R) with transient ligation of the left anterior descending (LAD) coronary artery in mice *in vivo*, global I/R in isolated perfused murine hearts *ex vivo*, and hypoxia/reoxygenation (H/R) in cell cultures *in vitro*. Next, we determined the regulation of SGLT1 during cardiac ischaemia. AMPK up-regulates SGLT1 through extracellular signal-related kinase (ERK) and RNA-binding protein HuR. Finally, we determined that SGLT1 contributes to ischaemic injury by interacting with epidermal growth factor receptor (EGFR), which in turn increases PKC and NADPH oxidase 2 (Nox2) activities and production of reactive oxygen species (ROS).

2. Methods

For detailed experimental procedures, see Supplementary material online.

2.1 Mouse models

All studies involving mice conformed to the *Guide for the Care and Use of Laboratory Animals* (NIH Publication No. 85-23, revised 1996) and were approved by the University of Pittsburgh and the University of Iowa Institutional Animal Care and Use Committees. Friend leukemia virus B (FVB/N) strain transgenic mice with cardiomyocyte-specific RNA interference knockdown of SGLT1 ($TG^{SGLT1\text{-}DOWN}$) were constructed as we have previously reported.[16] Equal proportions of male and female $TG^{SGLT1\text{-}DOWN}$ 6- to 8-week-old mice (20–25 g body mass) and wild-type littermates were used for all *ex vivo* and *in vivo* experiments. Mice underwent *in vivo* ischaemia for 30 min by ligation of the LAD coronary artery. Isolated perfused hearts underwent *ex vivo* ischaemia with either 20 min of zero-flow (ischaemia) followed by up to 120 min of re-flow (reperfusion), or continuous flow. Eighty out of a total of 113 mice were used in the final data analysis. Mice that did not survive *in vivo* surgery and those with a low intrinsic heart rate (<300/min) in *ex vivo* Langendorff isolated perfused heart preparations were excluded from the study. There were no significant differences among experimental groups in the proportion of excluded mice. Mice were anaesthetized with ketamine (87.5 mg/kg) and xylazine (12.5 mg/kg) administered intraperitoneally once. Mice were euthanized using CO_2 inhalation and cervical dislocation.

2.2 *In vitro* HL-1 cell and isolated murine ventricular cardiomyocyte culture studies

The HL-1 cardiac cell line derived from murine atrial cardiomyocytes (a generous gift from William C. Claycomb, PhD, Louisiana State University)[17] and isolated adult murine ventricular cardiomyocytes were used for *in vitro* studies as described in the Supplementary material online.

2.3 Statistical analysis

Individual data and mean ± standard error are presented in the graphs. Comparisons between two groups were made using the Student's *t*-test. For comparisons among three or more groups, one-way analysis of variance (ANOVA) was used, followed by *post hoc* Bonferroni correction. A *P*-value <0.05 was considered significant.

3. Results

3.1 SGLT1 is up-regulated in ischaemia–reperfusion and knockdown of SGLT1 is protective against injury

Wild-type and $TG^{SGLT1\text{-}DOWN}$ hearts *ex vivo* exhibited similar AMPK activity at baseline, as reflected by Thr^{172} phosphorylation (p-AMPK), and a similar increase in AMPK activity following ischaemia that persisted after reperfusion (I/R) (Supplementary material online, *Figure S1A* and *B*). Wild-type hearts exhibited an increase in SGLT1 mRNA and protein expression after ischaemia that was markedly attenuated in $TG^{SGLT1\text{-}DOWN}$ hearts (Supplementary material online, *Figure S1C* and *D*). Increased expression of SGLT1 protein was observed in *in vivo* and in *ex vivo* wild-type mouse hearts subjected to ischaemia followed by reperfusion (I/R) (*Figure 1A* and *B*). Compared to wild-type mice, decreased SGLT1 expression was observed in $TG^{SGLT1\text{-}DOWN}$ mice both at baseline and following I/R (*Figure 1A* and *B*). In both *in vivo* and *ex vivo* I/R models, relative to wild-type hearts, $TG^{SGLT1\text{-}DOWN}$ hearts exhibited significantly smaller infarct sizes (*Figure 1C*). Of note, the area at risk was similar between wild-type and $TG^{SGLT1\text{-}DOWN}$ mice at baseline prior to *in vivo* I/R (Supplementary material online, *Figure S1E*). $TG^{SGLT1\text{-}DOWN}$ hearts exhibited significantly less release of creatine kinase following *ex vivo* I/R, reflecting less myocardial injury (*Figure 1D*). In addition, production of malondialdehyde (MDA), a marker of lipid peroxidation and oxidative stress, was significantly decreased in $TG^{SGLT1\text{-}DOWN}$ hearts following *in vivo* and *ex vivo* I/R (*Figure 1E*). There was also evidence that SGLT1 knockdown led to preserved systolic and diastolic function with reperfusion. At baseline, there were no differences between wild-type and $TG^{SGLT1\text{-}DOWN}$ hearts in *ex vivo* coronary flow, spontaneous heart rate, rate pressure product, left end-diastolic pressure, and $+dP/dt_{max}$ (Supplementary material online, *Table S1*). In *ex vivo,* isolated

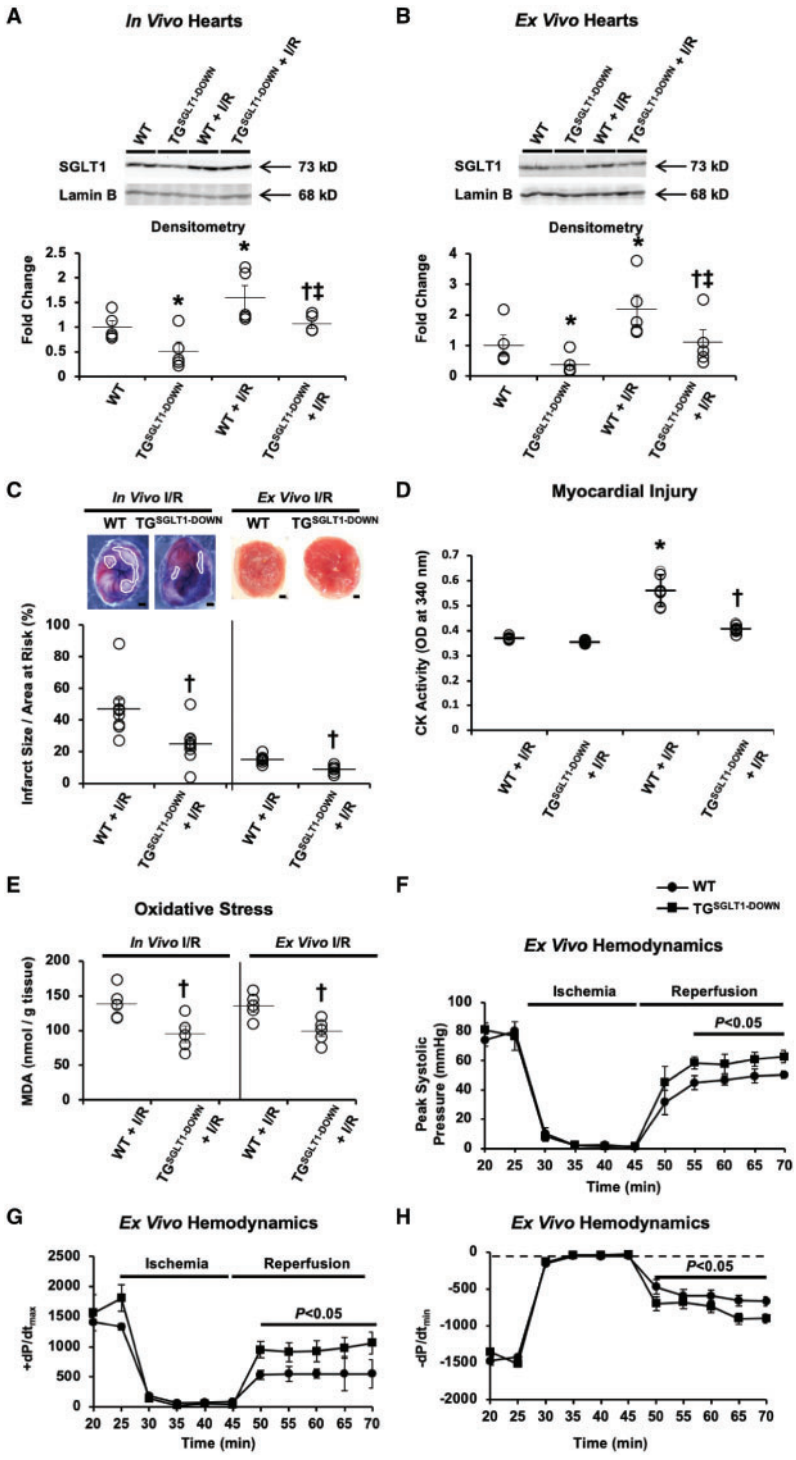

Figure 1 Decreased injury following I/R after knockdown of SGLT1 in *in vivo* and *ex vivo* models. (*A* and *B*) Protein level of SGLT1 in $TG^{SGLT1\text{-}DOWN}$ hearts relative to wild-type (WT) hearts. Representative immunoblots are shown on the top and densitometry data on the bottom. Lamin B was used as a loading control. $n = 5$/group. (*C*) Triphenyl tetrazolium chloride-stained tissue sections from WT and $TG^{SGLT1\text{-}DOWN}$ hearts. Representative images are shown on the top and infarct size quantified as ratio of infarct area to area at risk (AAR) are shown on the bottom. The surface of the heart slices that were considered to be infracted are demarcated by white lines. Scale bars equal 500 µm. $n = 5$/group. (*D*) Coronary effluent was collected after reperfusion of 10 min during *ex vivo* I/R, and creatine kinase activity measured. (*E*) Oxidative stress following I/R, quantified by MDA content in cardiac tissue. $n = 5$/group. (*F–H*) Left ventricular peak systolic pressure, $+dP/dt_{max}$, and $-dP/dt_{min}$ in $TG^{SGLT1\text{-}DOWN}$ and WT hearts during *ex vivo* I/R. $n = 8$–10/group. $^{*}P < 0.05$ vs. WT control; $^{\dagger}P < 0.05$ vs. WT I/R; $^{\ddagger}P < 0.05$ vs. $TG^{SGLT1\text{-}DOWN}$ control. Data shown in panels *A*, *B*, and *D* were analysed for statistical significance using one-way ANOVA followed by *post hoc* Bonferroni correction. Data shown in panels *C*, *E*, *F*, *G*, and *H* were analysed for statistical significance using the Student's *t*-test.

$TG^{SGLT1\text{-}DOWN}$ but not wild-type hearts, peak left ventricular systolic pressure recovered to baseline after reperfusion, and $+dP/dt_{max}$ and $-dP/dt_{min}$ were partially preserved (*Figure 1F–H*).

These differences were unrelated to differences in glucose transportation by either the GLUTs or SGLT1. As we have previously reported,[16] cardiac GLUT1 and GLUT4 protein expression was unchanged in $TG^{SGLT1\text{-}DOWN}$ mice relative to wild-type littermates (Supplementary material online, *Figure S2A*). We measured glucose uptake *ex vivo* in intact wild-type and $TG^{SGLT1\text{-}DOWN}$ hearts at baseline and after I/R (Supplementary material online, *Figure S2B*), and also in cardiomyocytes isolated from these hearts (Supplementary material online, *Figure S2C*). Both in intact *ex vivo* isolated perfused hearts and in isolated cardiomyocytes, there was no difference in glucose uptake between wild-type and $TG^{SGLT1\text{-}DOWN}$. Although there was an increase in glucose uptake after I/R, the increase was again similar between wild-type and $TG^{SGLT1\text{-}DOWN}$ intact hearts and isolated cardiomyocytes. The *ex vivo* experiments shown in *Figure 1* were performed using pyruvate in the perfusate. Similar differences between $TG^{SGLT1\text{-}DOWN}$ and wild-type hearts in infarct size, oxidative stress, and haemodynamics were observed when glucose was used in the perfusate (Supplementary material online, *Figure S3*). Finally, we repeated the *ex vivo* experiments using glucose in the perfusate, and extending reperfusion for 2 h. As in our prior experiments, $TG^{SGLT1\text{-}DOWN}$ hearts exhibited decreased infarct size and preserved cardiac function (Supplementary material online, *Figure S4A* and *B*).

Similarly, in HL-1 cells, H/R *in vitro* led to increased AMPK activity, as reflected by Thr^{172} phosphorylation (p-AMPK), and increased expression of SGLT1 (*Figure 2A*). Transfection of SGLT1 siRNA led to decreased expression of SGLT1 both at baseline and following H/R relative to control cells transfected with scrambled siRNA. However, AMPK activity was similar in SGLT1 siRNA and scrambled siRNA transfected cells at baseline, and increased similarly in both groups of cells following H/R. Furthermore, the increase in SGLT1 expression following H/R was abolished by the AMPK inhibitor compound C (*Figure 2B*). Knockdown of SGLT1 improved cell viability following H/R (*Figure 2C*), decreased injury as reflected by lactate dehydrogenase (LDH) release (*Figure 2D*), and decreased oxidative stress as reflected by MDA production (*Figure 2E*). Thus, *in vivo*, *ex vivo*, and *in vitro* studies all showed that SGLT1 knockdown was protective against ischaemic injury.

3.2 Regulation of SGLT1 in cardiac ischaemia

During cardiac ischaemia, AMPK is activated by Thr^{172} phosphorylation (p-AMPK)[18] (see also Supplementary material online, *Figure S1*). Exposure of HL-1 cells to the AMPK activator metformin increased expression of p-AMPK and SGLT1 protein (*Figure 3A*). These effects were abrogated by the AMPK inhibitor compound C. SiRNA-mediated knockdown of either the α1 or the α2 catalytic subunit of AMPK attenuated the up-regulation of SGLT1 protein in the presence of metformin (Supplementary material online, *Figure S5A* and *B*). However, only AMPK α2 subunit knockdown abolished up-regulation of SGLT1 following H/R (Supplementary material online, *Figure S5C* and *D*). These findings suggest that the α2 subunit of AMPK is the specific isoform responsible for up-regulation of SGLT1 following H/R. Oxidative stress (Supplementary material online, *Figure S5E*) and cell viability (Supplementary material online, *Figure S5F*) following H/R were unaltered by either AMPK α1 or AMPK α2 knockdown. The lack of an effect on cell viability and oxidative stress may be related to the fact that AMPK has multiple targets in addition to SGLT1, many of which, unlike SGLT1, may be cardioprotective during ischaemia.

Co-immunoprecipitation studies using protein from isolated perfused hearts with or without I/R showed that, although AMPK does not interact with SGLT1, ERK interacts with both AMPK and SGLT1 (*Figure 3B*), suggesting that ERK may act as an intermediary in the up-regulation of SGLT1 by AMPK. Consistent with this hypothesis, metformin led to an increase in activated, phosphorylated ERK (p-ERK) and SGLT1 mRNA, and protein expression in isolated adult murine ventricular cardiomyocytes (*Figure 3C* and *D*). Exposure of HL-1 cells to both metformin and the ERK inhibitor U0126 abrogated the increased expression of activated, phosphorylated ERK (p-ERK) and SGLT1, but had no effect on the expression of activated, phosphorylated AMPK (p-AMPK) (*Figure 3E*).

The promoter of the gene encoding SGLT1 (*SLC5A1*) contains two binding sites for specificity protein 1 (Sp1) and one for hepatocyte nuclear factor 1 (HNF-1) that increase transcription.[19] The protein HuR increases SGLT1 mRNA stability by binding to a critical uridine-rich element in its 3' untranslated region (3'-UTR).[20] AMPK stimulates binding of HuR to its targets[21] and ERK2 targets HuR.[22] Metformin increased binding of Sp1, HNF-1, and HuR to their respective targets in HL-1 cells, effects that were abrogated by the AMPK inhibitor compound C (*Figure 4A–C*). Sp1 can be phosphorylated by several kinases, including ERK, that enhances its binding activity.[23] Mirk, a dimerization cofactor of HNF-1, is activated by phosphorylation and subsequently stabilizes HNF-1 and enhances its transcriptional activity.[24] The AMPK activator metformin increased phosphorylation of HuR, Sp1, and Mirk, and nuclear localization of HNF-1 in HL-1 cells (*Figure 4D*). These effects were attenuated or abrogated by the ERK inhibitor U0126. Exposure of HL-1 cells to siRNA targeting HNF-1, Sp1, and HuR successfully decreased expression of the targets (*Figure 4E–G*), but only HuR knockdown resulted in decreased expression of SGLT1 mRNA (*Figure 4H*). HuR knockdown also impaired SGLT1 mRNA stability, consistent with the function of HuR, whereas HNF-1 and Sp1 knockdown had no effect on SGLT1 mRNA stability (*Figure 4I*).

In non-cardiac tissues, phosphorylation of SGLT1 has been shown to cause its translocation from intracellular vesicles to the cell membrane and an increase in glucose uptake.[25] Our studies suggested that a similar mechanism exists in cardiomyocytes. In HL-1 cells, the AMPK activator metformin increased phosphorylation of SGLT1, an effect that was reversed in the presence of the ERK inhibitor U0126 (*Figure 5A*). Immunoblots of membrane and cytosolic protein fractions from HL-1 cells showed that metformin increased expression of SGLT1 in the membrane fraction, an effect that was abolished by U0126 (*Figure 5B*). Consistent with this finding, immunofluorescence studies showed that the phosphorylation of SGLT1 was correlated with translocation to the sarcolemma (*Figure 5C*). Co-immunoprecipitation studies of cardiac protein from wild-type isolated perfused hearts with or without I/R showed no interaction between SGLT1 and caveolin-3 (*Figure 5D*), suggesting that caveolin-3 is not directly involved in trafficking of SGLT1 to the sarcolemma.

Thus, collectively, our data suggest that AMPK activates ERK, which in turn increases expression of SGLT1 protein through Sp1 and HNF-1, and increases transcript stability through HuR. Furthermore, ERK phosphorylates SGLT1 and causes its translocation to the sarcolemma.

3.3 Activation of PKC and p47phox by SGLT1

Following *ex vivo* I/R of isolated perfused hearts, $TG^{SGLT1\text{-}DOWN}$ hearts, relative to wild-type hearts, exhibited decreased expression of total

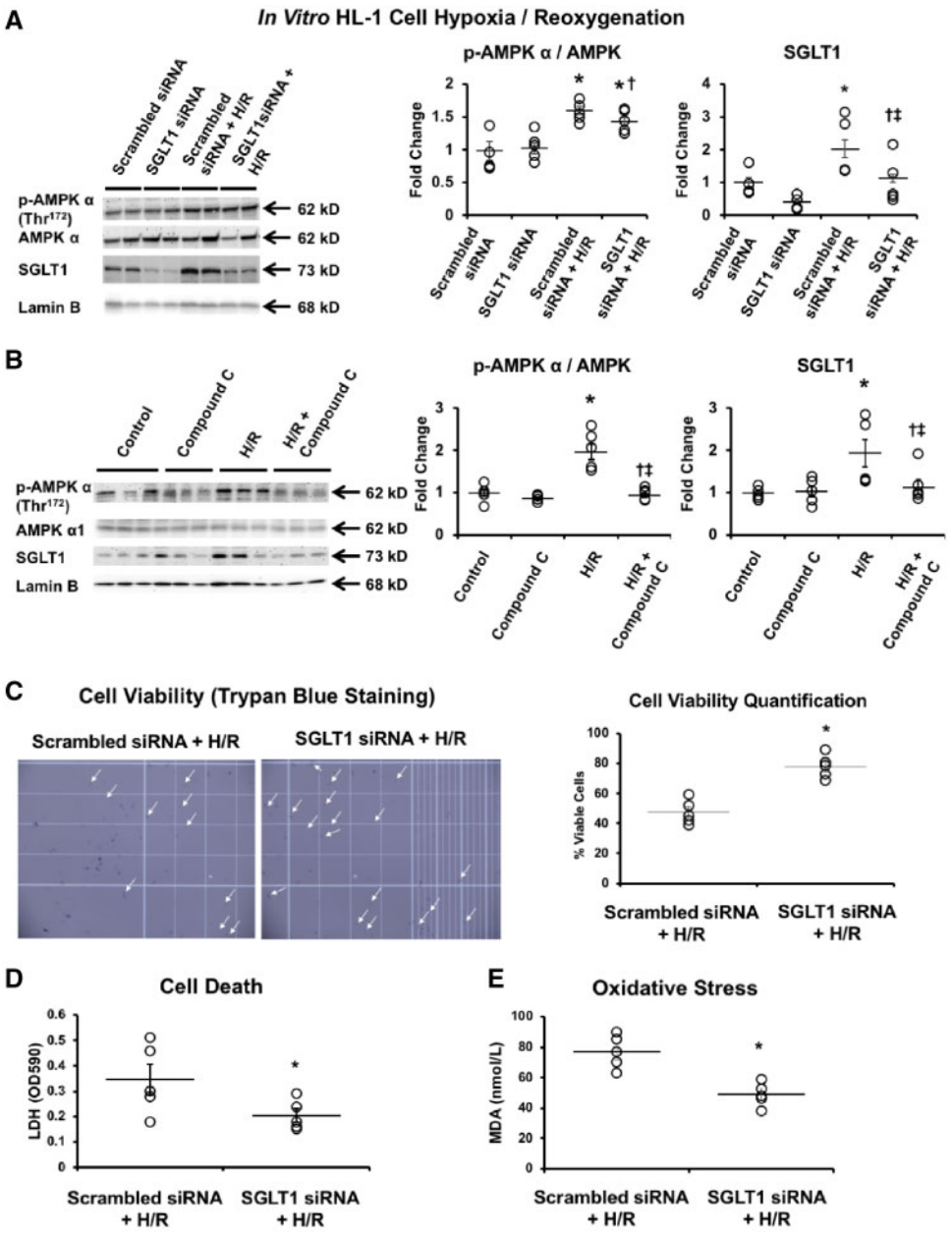

Figure 2 Decreased injury following exposure of HL-1 cells to *in vitro* H/R was observed following knockdown of SGLT1. (*A*) Protein expression of Thr^{172} phosphorylated AMPK α subunit (p-AMPK α), total AMPK, and SGLT1 in HL-1 cells transfected with SGLT1 siRNA relative to HL-1 cells transfected with scrambled siRNA. Lamin B was used as a loading control. Four independent experiments were performed. $n = 5$/group. $^{*}P < 0.05$ vs. scrambled siRNA; $^{\dagger}P < 0.05$ vs. scrambled siRNA + H/R; $^{\ddagger}P < 0.01$ vs. SGLT1 siRNA. (*B*) Protein expression of Thr^{172} phosphorylated AMPK α subunit (p-AMPK α), total AMPK and SGLT1 in HL-1 cells treated with or without the AMPK inhibitor compound C (10 μM) and exposed to normoxia or H/R. Lamin B was used as a loading control. $n = 5$/group. $^{*}P < 0.05$ vs. control; $^{\dagger}P < 0.05$ vs. H/R; $^{\ddagger}P < 0.01$ vs. compound C. Data were analysed for statistical significance using one-way ANOVA followed by *post hoc* Bonferroni correction. (*C*) Cell viability in HL-1 cells transfected with SGLT1 siRNA or scrambled siRNA and exposed to H/R, assessed by trypan blue exclusion. $n = 5$/group. Representative scans are shown, in which surviving cells are unstained (indicated by white arrows) and non-viable cells are stained blue. $^{*}P < 0.05$ vs. scrambled siRNA + H/R. (*D*) Cell death following H/R, assessed by lactate dehydrogenase (LDH) release. $n = 5$/group. $^{*}P < 0.05$ vs. scrambled siRNA + H/R. (*E*) Oxidative stress following H/R, quantified by MDA content in cardiac tissue. $n = 5$/group. $^{*}P < 0.05$ vs. scrambled siRNA + H/R. Data shown in panels *A* and *B* were analysed for statistical significance using one-way ANOVA followed by *post hoc* Bonferroni correction. Data shown in panels *C*, *D*, and *E* were analysed for statistical significance using the Student's *t*-test.

phosphorylated, activated PKC (p-PKC) and of the PKCβ and the PKCδ isoforms (*Figure 6A*). PKC leads to phosphorylation of p47phox, which in turn leads to activation of Nox2. TG$^{\text{SGLT1-DOWN}}$ hearts, relative to wild-type hearts, exhibited decreased relative phosphorylation of p47phox (*Figure 6A*).

HL-1 cells were subjected to H/R or were transfected with SGLT1 cDNA expression vectors. Either condition resulted in increased cellular expression of SGLT1 or total phosphorylated PKC, and membrane expression of p47phox and Nox2 (*Figure 6B*). Administration of the PKC

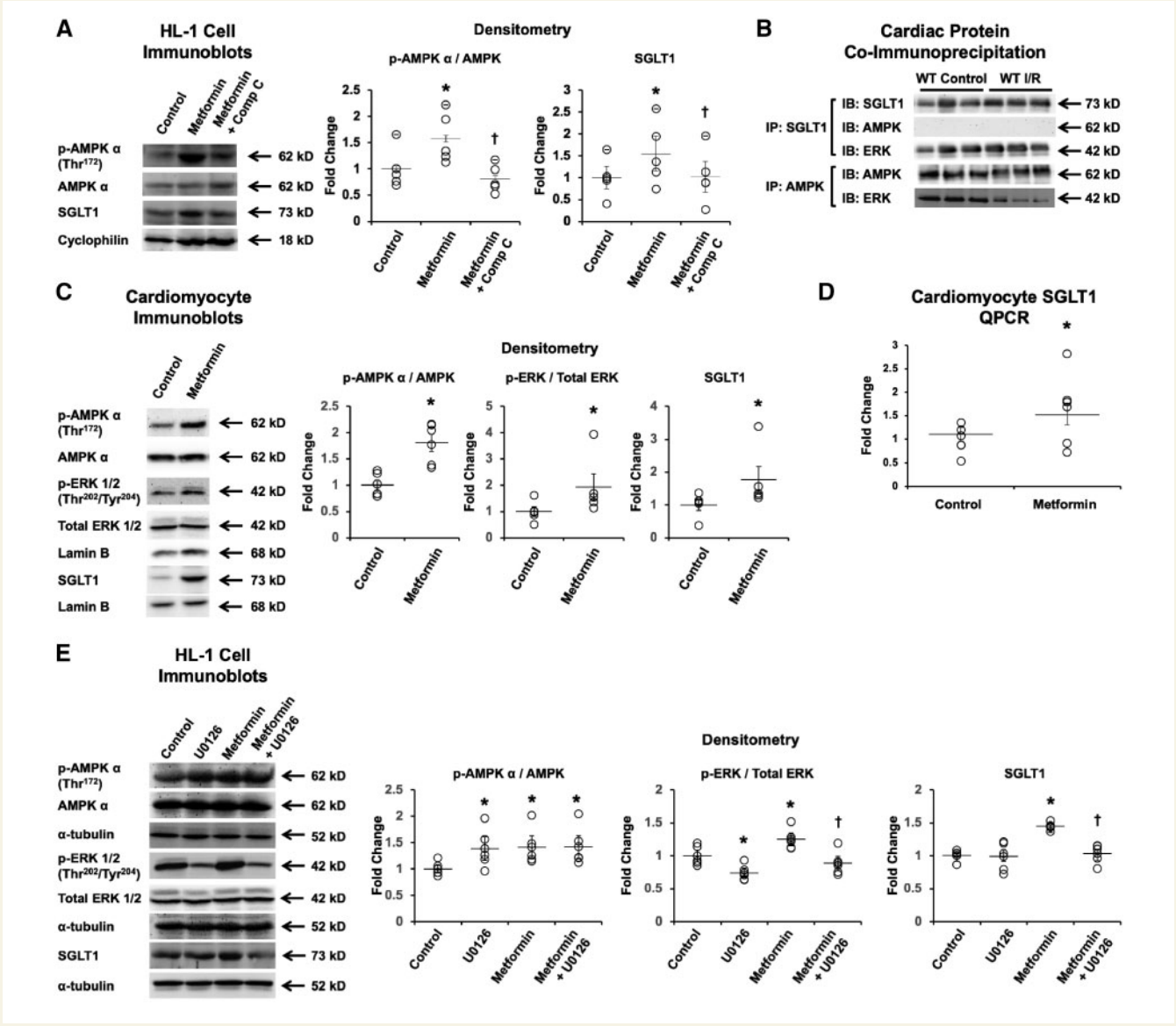

Figure 3 During ischaemia, AMPK up-regulates SGLT1 via ERK. (*A*) HL-1 cells were treated with vehicle alone (0.1% DMSO, control), the AMPK activator metformin (2 mM), and/or the AMPK inhibitor compound C (Comp C, 10 μM) for 25 h. Representative immunoblots and denstiometry analyses are shown of protein expression of Thr^{172} phosphorylated AMPK α subunit (p-AMPK α), total AMPK α, and SGLT1 relative to control. Cyclophilin was used as a loading control. $n = 5$/group. $^{*}P < 0.05$ vs. control; $^{\dagger}P < 0.05$ vs. metformin. (*B*) Co-immunoprecipitation analyses of SGLT1, AMPK, and ERK in total cardiac protein from wild-type hearts exposed to *ex vivo* continuous perfusion (control) or I/R. $n = 5$/group. (*C* and *D*) Isolated adult murine ventricular cardiomyocytes were treated with vehicle alone (0.1% DMSO, control), or the AMPK activator metformin (2 mM) for 25 h. Protein expression of Thr^{172} phosphorylated AMPK α subunit (p-AMPK α), total AMPK α, and SGLT1 were assessed by immunoblot (*C*) and SGLT1 mRNA relative to control by QPCR (*D*). Lamin B was used as a loading control for the immunoblots. $n = 5$/group. $^{*}P < 0.05$ vs. control. Data were analysed for statistical significance using the Student's *t*-test. (*E*) HL-1 cells were treated with vehicle alone (0.1% DMSO, control), metformin (2 mM), and/or the ERK inhibitor U0126 (1 μM) for 25 h. Representative immunoblots and denstiometry analyses are shown of protein expression of p-AMPK α subunit, total AMPK α subunit, phosphorylated ERK1/2 (Thr^{202}/Tyr^{204}), and SGLT1. α-tubulin was used as a loading control. $n = 5$/group. $^{*}P < 0.01$ vs. control; $^{\dagger}P < 0.05$ vs. metformin. Data were analysed for statistical significance using one-way ANOVA followed by *post hoc* Bonferroni correction.

inhibitor chelerythrine concurrent with H/R or forced expression of SGLT1 attenuated or abrogated the increases in expression of total phosphorylated PKC, p47phox, and Nox2. Increased oxidative stress, assessed by MDA production (*Figure 6C*) and cell death, assessed by LDH production (*Figure 6D*), induced by forced expression of SGLT1 was attenuated by the Nox2 inhibitor gp91 dstat.

3.4 EGFR serves as a mediator between SGLT1 and PKC

Co-immunoprecipitation studies of cardiac protein from wild-type isolated perfused hearts with or without I/R showed that EGFR interacts with both SGLT1 and PKC, but that SGLT1 does not directly interact with PKC (*Figure 7A*). In HL-1 cells exposed to the AMPK activator

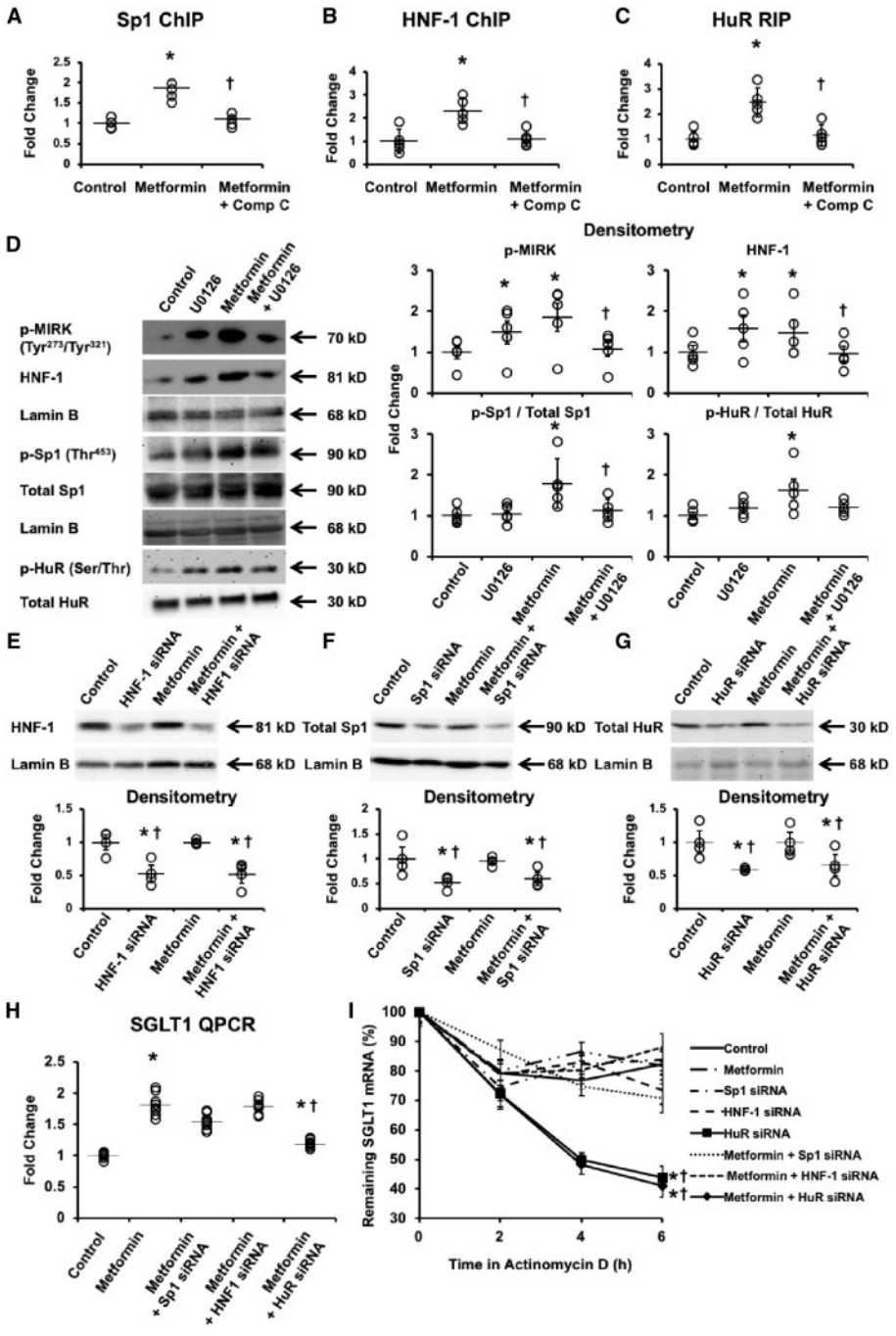

Figure 4 Transcriptional and post-translational up-regulation of SGLT1. (*A–C*) HL-1 cells were exposed to 0.1% DMSO vehicle alone (control), metformin (2 mM), or metformin and compound C (Comp C, 10 μM) for 25 h. HNF-1 and Sp1 binding to the promoter of the SGLT1 gene (*Slc5a1*) and HuR binding to the 3'-UTR of SGLT1 mRNA were quantified by ChIP and RIP, respectively. $n = 5$/group. $^{*}P < 0.01$ vs. control; $^{\dagger}P < 0.05$ vs. metformin. (*D*) HL-1 cells were exposed to 0.01% DMSO vehicle alone (control), U0126 (1 μM), metformin (2 mM), or metformin and U0126 for 25 h. $n = 3$/group. Left, representative immunoblots of Tyr^{273}/Tyr^{321}-phosphorylated Mirk, Thr^{453}-phosphorylated Sp1 (p-Sp1), total Sp1, Ser/Thr phosphorylated HuR (p-HuR), total HuR, and nuclear HNF-1. Lamin B was used as a loading control. Right, densitometry analyses. $n = 5$/group. $^{*}P < 0.05$ vs. control; $^{\dagger}P < 0.05$ vs. metformin. (*E–H*) HL-1 cells were transfected with siRNA knocking down HNF-1, Sp1, or HuR, followed by exposure to metformin (2 mM) or vehicle for 24 h. Control cells were transfected with scrambled siRNA. Representative immunoblots of protein expression of HNF-1 (*E*), Sp1 (*F*), and HuR (*G*) are shown in the top panels and densitometry analyses in the bottom panels. Lamin B was used as a loading control. $n = 4$/group. $^{*}P < 0.01$ vs. control; $^{\dagger}P < 0.05$ vs. metformin. Expression of SGLT1 mRNA was assessed by QPCR (*H*). $n = 7$/group. (*I*) HL-1 cells were transfected with siRNA knocking down HNF-1, Sp1, or HuR, treated with vehicle alone (0.1% DMSO, control) or metformin (2 mM), and finally exposed to actinomycin D (1 μM) or 0.1% DMSO for 2, 4, or 6 h. Control cells were transfected with scrambled siRNA. SGLT mRNA was measured by QPCR. $n = 3$/group. $^{*}P < 0.01$ vs. control; $^{\dagger}P < 0.05$ vs. metformin. Data were analysed for statistical significance using one-way ANOVA followed by *post hoc* Bonferroni correction.

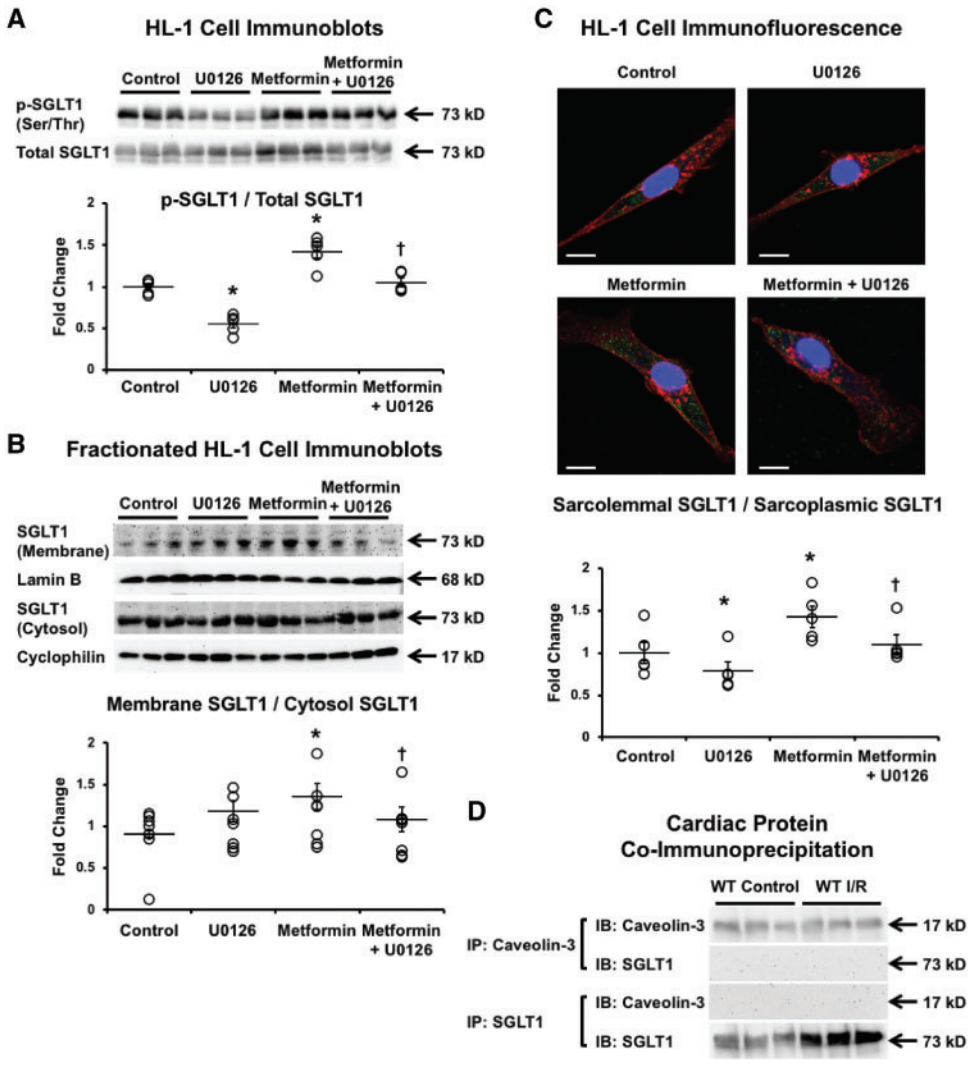

Figure 5 SGLT1 phosphorylation leads to translocation to the cell surface. HL-1 cells were treated with vehicle alone (0.1% DMSO, control), metformin (2 mM), compound C (Comp C, 10 μM), and/or U0126 (1 μM) for 25 h. (*A*) SGLT1 was immunoprecipitated and subjected to a pan-phosphoserine/threonine antibody to quantify relative SGLT1 phosphorylation. The top panels show representative immunoblots and the bottom panels show densitometry analyses. $n = 5$/group. $^{*}P < 0.01$ vs. control; $^{\dagger}P < 0.05$ vs. metformin. (*B*) Protein expression of SGLT1, lamin B, and cyclophilin were determined by immunoblot. The top panels show representative immunoblots and the bottom panels show densitometry analyses. $n = 5$/group. $^{*}P < 0.01$ vs. control; $^{\dagger}P < 0.05$ vs. metformin. (*C*) Top, representative immunofluorescence images showing localization of SGLT1. Green, SGLT1; red, wheat germ agglutinin, sarcolemma; blue, DAPI, nuclei. Scale bar equals 20 μm. Bottom, SGLT1 translocation was quantified as ratio of sarcolemma to sarcoplasm. $n = 5$/group. $^{*}P < 0.05$ vs. control; $^{\dagger}P < 0.05$ vs. metformin. Data shown in panels *A*, *B*, and *C* were analysed for statistical significance using one-way ANOVA followed by *post hoc* Bonferroni correction. (*D*) Cardiac protein from isolated perfused wild-type mouse hearts exposed to normal flow (control) or *ex vivo* I/R were immunoprecipitated with anti-caveolin-3 or anti-SGLT1 antibodies, and the immunoprecipitates probed on immunoblots for caveolin-3 or SGLT1. A representative immunoblot is shown. $n = 5$/group.

metformin, there was increased interaction of SGLT1 with the active, Tyr^{1173}-phosphorylated form of EGFR (p-EGFR, *Figure* 7*B*). This interaction was abolished by the ERK inhibitor U0126 (*Figure* 7*B*). Transfection of HL-1 cells with an SGLT1 cDNA expression vector resulted in increased expression of SGLT1 and phosphorylated PKC (p-PKC) (*Figure* 7*C*). The EGFR inhibitor gefitinib treatment had no effect on SGLT1 expression, but abolished increased PKC phosphorylation associated with SGLT1 overexpression. These findings suggested that EGFR mediates PKC activation by SGLT1.

SGLT1 interacts with the autophosphorylation domain of EGFR.[26] To determine whether PKC activation requires direct interaction between SGLT1 and EGFR, we co-transfected HL-1 cells with combinations of expression vectors as listed below, followed by exposure to normoxia or H/R. Control cells were transfected with an equal amount of Myc-tagged and HA-tagged empty vectors. SGLT1 cDNA cells were transfected with SGLT1 cDNA containing a Myc tag and an empty vector containing an HA tag. H/R + WT EGFR cells were transfected with an empty vector containing a Myc tag and a wild type sequence EGFR

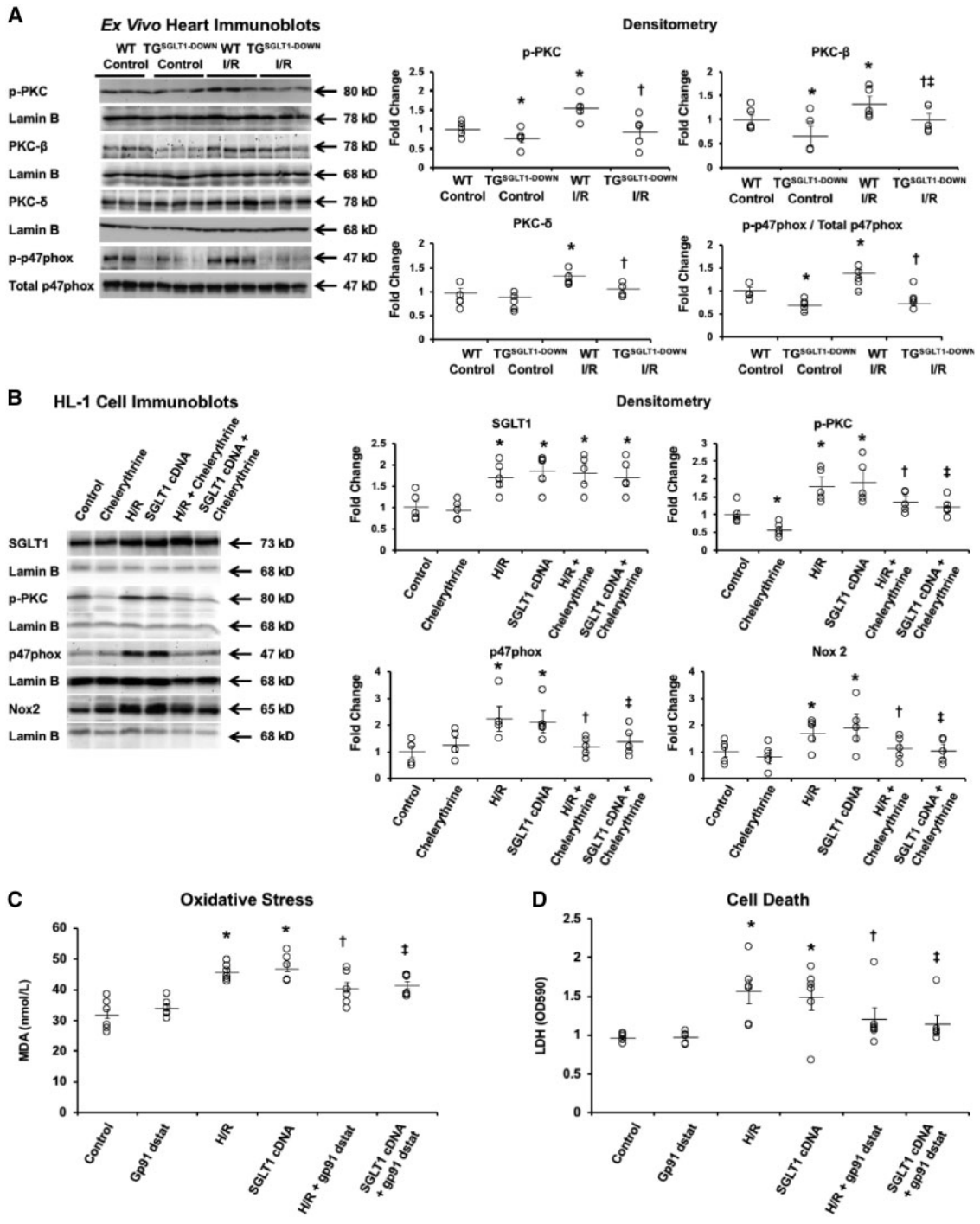

Figure 6 SGLT1 up-regulation leads to activation of PKC and Nox2. (*A*) Isolated perfused WT and TG$^{SGLT1\text{-}DOWN}$ hearts were exposed to continuous flow (control) or no-flow I/R. Representative immunoblots are shown of phosphorylated PKC (p-PKC), PKC β, PKC δ, phosphorylated (p-p47phox), and total p47phox. Lamin B was used as a loading control. Representative immunoblots and densitometry analyses are shown. $n = 5$/group. $^{*}P < 0.05$ vs. WT control; $^{\dagger}P < 0.05$ vs. WT I/R; $^{\ddagger}P < 0.05$ vs. TG$^{SGLT1\text{-}DOWN}$ control. (*B*) HL-1 cells were transfected with an empty expression vector (control), exposed to H/R, or transfected with a SGLT1 cDNA expression vector (SGLT1 cDNA). Cells were also treated with or without the PKC inhibitor chelerythrine (1 μM). Representative immunoblots and densitometry analyses are shown of SGLT1, p-PKC, Nox2, and p47phox. $n = 5$/group. $^{*}P < 0.01$ vs. control; $^{\dagger}P < 0.05$ vs. H/R; $^{\ddagger}P < 0.05$ vs. SGLT1 cDNA. (*C* and *D*) HL-1 cells were transfected with an empty expression vector (control), exposed to H/R, or transfected with a SGLT1 cDNA expression vector (SGLT1 cDNA). Cells were also treated with or without the Nox2 inhibitor gp91 dstat (5 μM) for 25 h. (*C*) Oxidative stress following H/R, quantified by MDA in the cell lysate. $n = 5$/group. (*D*) Cell death following H/R, assessed by LDH release. $n = 5$/group. $^{*}P < 0.01$ vs. control; $^{\dagger}P < 0.05$ vs. H/R; $^{\ddagger}P < 0.05$ vs. SGLT1 cDNA. Data were analysed for statistical significance using one-way ANOVA followed by *post hoc* Bonferroni correction.

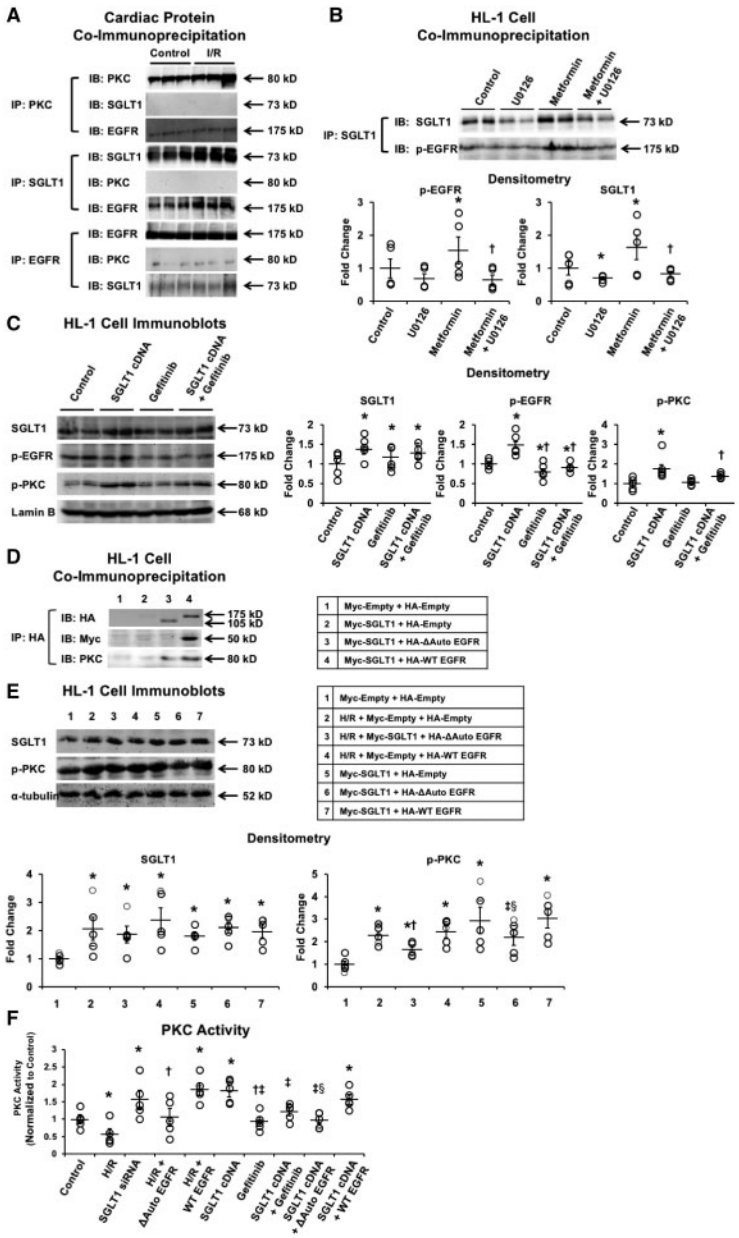

Figure 7 EGFR mediates activation of PKC by SGLT1. (*A*) Cardiac protein from isolated perfused wild-type mouse hearts exposed to normal flow (control) or no-flow I/R were immunoprecipitated with anti-PKC (upper panel), anti-SGLT1 (middle panel), and anti-EGFR (lower panel) primary antibodies, and the immunoprecipitate samples probed on immunoblots for SGLT, EGFR, and PKC. $n = 5$/group. (*B*) HL-1 cells were treated with vehicle alone (0.01% DMSO, control), U0126 (1 μM), metformin (2 mM), or metformin and U0126. Top, protein was immunoprecipitated with anti-SGLT1 primary antibody and the immunoprecipitate samples probed on immunoblots for SGLT1 and Tyr^{1173}-phosphorylated EGFR (p-EGFR); bottom, densitometry analyses. $n = 5$/group. $^{*}P < 0.05$ vs. control; $^{\dagger}P < 0.05$ vs. metformin. (*C*) HL-1 cells were transfected with an expression vector containing SGLT1 cDNA or an empty expression vector, and with or without the EGFR inhibitor gefitinib (1 μM). Left, protein was immunoblotted for SGLT1, Tyr^{1173}-phosphorylated EGFR (p-EGFR), phosphorylated PKC (p-PKC), and lamin B; right, densitometry analyses. $n = 5$/group. $^{*}P < 0.05$ vs. control; $^{\dagger}P < 0.05$ vs. SGLT1 cDNA. (*D–F*) HL-1 cells were transfected with SGLT1 siRNA in normoxic conditions, or transfected with combinations of expression vectors as listed below, followed by exposure to normoxia or H/R, in the presence or absence of gefitinib. Control cells were treated with an equal amount of Myc tagged and HA tagged empty vectors. SGLT1 cDNA cells were transfected with SGLT1 cDNA containing a Myc tag and an empty vector containing an HA tag. H/R + WT EGFR cells were transfected with an empty vector containing a Myc tag and a wild-type EGFR vector containing an HA tag. H/R + mutant EGFR (ΔAuto EGFR) cells were transfected with an empty vector containing a Myc tag and a mutant EGFR (ΔAuto EGFR) vector containing an HA tag. (*D*) Protein was immunoprecipitated with anti-HA primary antibody and the immunoprecipitate samples probed on immunoblots for HA, Myc, and PKC. $n = 5$/group. (*E*) Immunoblots were performed for SGLT1, phosphorylated PKC (p-PKC), and α-tubulin. Representative immunoblots and densitometry analyses are shown. $n = 5$/group. $^{*}P < 0.05$ vs. control; $^{\dagger}P < 0.05$ vs. H/R; $^{\ddagger}P < 0.05$ vs. SGLT1 cDNA; $^{\S}P < 0.05$ vs. SGLT1 cDNA + WT EGFR. (*F*) PKC activity was assayed in cells following the indicated treatments. $n = 5$/group. $^{*}P < 0.05$ vs. control; $^{\dagger}P < 0.05$ vs. H/R; $^{\ddagger}P < 0.05$ vs. SGLT1 cDNA; $^{\S}P < 0.05$ vs. SGLT1 cDNA + WT EGFR. Data were analysed for statistical significance using one-way ANOVA followed by *post hoc* Bonferroni correction.

vector containing an HA tag. H/R + mutant EGFR (ΔAuto EGFR) cells were transfected with an empty vector containing a Myc tag and a mutant EGFR (ΔAuto EGFR, lacking the autophosphorylation domain) vector containing an HA tag. Co-expression of SGLT1 and WT EGFR resulted in their direct interaction as documented by co-immunoprecipitation assays, and direct interaction between EGFR and PKC (*Figure 7D*). In contrast, SGLT1 did not interact with mutant EGFR (ΔAuto EGFR), and consequently there was decreased interaction between PKC and mutant EGFR (*Figure 7D*). Expression of active, phosphorylated PKC was increased in cells exposed to H/R or forced expression of SGLT1, an effect that was abrogated with concurrent expression of mutant EGFR (ΔAuto EGFR) (*Figure 7E*). PKC activity was increased in cells exposed to H/R or forced expression of SGLT1, an effect that was abrogated by the EGFR inhibitor gefitinib or by expression of mutant EGFR (ΔAuto EGFR) (*Figure 7F*). PKC activity was decreased by siRNA-mediated knockdown of SGLT1. Therefore, activation of PKC is dependent on activation of EGFR by interaction of its autophosphorylation domain with SGLT1.

4. Discussion

Our studies show that RNAi-mediated knockdown of SGLT1 in cardiomyocytes is protective against I/R injury in mice *in vivo*, in isolated perfused murine hearts *ex vivo*, and in isolated cells *in vitro*. SGLT1 knockdown is associated with decreased oxidative stress, decreased myocardial necrosis, smaller infarct sizes, and improved hemodynamic function after I/R or H/R injury. Collectively, these studies suggest that SGLT1 contributes to I/R injury. Activation of AMPK during cardiac I/R increases expression of SGLT1 and cause its translocation to the sarcolemma potentially by several mechanisms. First, the promoter of the gene encoding SGLT1 (*Slc5a1*) contains three *cis* elements that increase transcription—one binding site for HNF-1 and two binding sites for Sp1.[19] AMPK leads to increased binding HNF-1 and Sp1 to the *Slc5a1* promoter, thereby increasing expression of the gene. Second, AMPK stimulates binding of the protein HuR to a critical uridine-rich element in its 3'-UTR in the SGLT1 mRNA, which is known to increase its stability.[31] Activation of ERK by AMPK leads to increased phosphorylation of Sp1, HuR, and the HNF-1 co-factor Mirk which may be responsible for increased SGLT1 expression at both the transcript and the protein level. Third, ERK increases phosphorylation of SGLT1, which causes its translocation to the sarcolemma. Up-regulation of SGLT1 leads to increased binding to the autophosphorylation domain of EGFR, which in turn activates PKC. Subsequently, p47phox, a subunit of Nox2, is phosphorylated, leading to oxidative stress. Supplementary material online, *Figure S6* illustrates the mechanisms by which SGLT1 contributes to cardiac I/R injury.

Studies by other investigators in both cardiac and non-cardiac tissues corroborate some of the mechanisms that we have uncovered. AMPK is activated during cardiac ischaemia.[27] ERK has recently emerged as an important downstream signalling pathway of AMPK.[28,29] Sp1 can be phosphorylated by several kinases, including ERK, which enhances its binding activity.[30] Activation of Mirk by phosphorylation by ERK2 stabilizes HNF-1 and enhances its transcriptional activity.[24] In renal cells, HuR binds to the SGLT1 mRNA 3'-UTR and can increase its half-life of SGLT1 mRNA by protecting it from degradation.[20] It is reported that ERK regulates binding of HuR to its target mRNA.[22] In non-cardiac tissues, phosphorylation of SGLT1 has been shown to cause its translocation from intracellular vesicles to the cell membrane and an increase in glucose uptake,[25] and SGLT1 can be phosphorylated by ERK.[30] In normal, ischaemic, and hypertrophic human cardiac tissue, increased SGLT1 expression at the sarcolemma of cardiomyoctyes was associated with increases in expression of active, phosphorylated AMPK and ERK.[31] Our studies demonstrate that ERK but not AMPK directly interacts with SGLT1. AMPK activation leads to increased phosphorylation of ERK, Mirk, Sp1, HuR, and SGLT1, which can be abolished or attenuated by the ERK inhibitor U0126. Hence, during ischaemia, AMPK activates SGLT1 through ERK. However, there is also conflicting evidence suggesting that AMPK negatively regulates ERK in cardiac fibroblasts[32] and B16F10 murine melanoma cells.[33] Thus, there may be differences among cell types and possibly species. Furthermore, different activators of AMPK vary in their ability to activate ERK in isolated cardiomyocytes in culture. Whereas AICAR and A769662 did not activate ERK in a prior study,[34] metformin activated ERK in a manner similar to our findings.[35]

Two recent studies have reported that phlorizin, a non-specific SGLT inhibitor, exacerbates cardiac I/R injury.[36,37] These reports are similar to our own unpublished data using phlorizin and seem to be inconsistent with our findings reported here using RNAi knockdown of SGLT1. It is possible that there are divergent effects of acute pharmacological inhibition of SGLT1 as contrasted with subacute (our *in vitro* studies) or chronic (our *ex vivo* and *in vivo* studies) RNAi knockdown of SGLT1. Furthermore, phlorizin can also inhibit the facilitative GLUT transporters. Indeed, decreased uptake of the glucose analogue 2-deoxy-D-glucose (2-DG) was found in the presence of phlorizin.[36,37] 2-DG is thought to be a poor substrate for SGLT1, suggesting that the increased I/R injury in the presence of phlorizin may in fact be secondary to inhibition of the GLUTs rather than SGLT1.

Oxidative stress is thought to be a key player in myocardial I/R injury. In the cardiovascular system, Nox accounts for a major proportion of ROS generation. Among five Nox isoforms, Nox2 is the only one expressed in cardiomyocytes. In our study, cardiomyocyte knockdown of SGLT1 led to decreased PKC and p47phox activation and ultimately decreased ROS production. Consistent with other investigators' findings,[30] we found no direct interaction between SGLT1 and PKC in the mouse heart. In cancer cells, SGLT1 is known to interact with and stabilize EGFR,[26] which in turn activates PKC.[38] Also, EGFR leads to increased mitochondrial ROS production,[39] which can directly activate PKC. We were able to confirm direct interaction between SGLT1 and EGFR as well as between EGFR and PKC in mouse hearts, which suggests that SGLT1 activates PKC through EGFR. Elevated glucose levels can increase PKC phosphorylation and activity.[40] However, we found no difference in GLUT1 and GLUT4 expression between wild-type and $TG^{SGLT1\text{-}DOWN}$ hearts. Glucose uptake was no different between wild-type and $TG^{SGLT1\text{-}DOWN}$ hearts both at baseline and after I/R. During *ex vivo* I/R, $TG^{SGLT1\text{-}DOWN}$ hearts showed decreased infarct size, reduced oxidative stress, and improved cardiac function regardless of whether pyruvate or glucose was present in the perfusate. These observations suggest that SGLT1 activates PKC independently of its glucose transport activity, by interacting with EGFR. The EGFR/PKC signalling pathway is documented to play an important role in many different disease states. However, a relationship between SGLT1 and PKC, through EGFR, has never been established previously.

Some prior studies have found that activation of AMPK inhibits Nox2 in cardiomyocytes, inconsistent with our model. Some of these studies have used AMPK activators that do not lead to ERK activation in cardiomyocytes. Thus, their effect on Nox2 may be mediated by AMPK targets

other than ERK and SGLT1. It is possible that AMPK, acting through other pathways, may attenuate Nox2 activation mediated by our postulated AMPK-ERK-SGLT1-EGFR-PKC-Nox2 pathway.

Different PKC isoforms have different effects on cardiac I/R injury and are active at distinct time points.[41] Inhibition of PKC β protects the heart against I/R injury by decreasing ROS production,[42,43] and inhibition of PKC δ prevents reperfusion injury.[41] In this study, $TG^{SGLT1\text{-}DOWN}$ hearts showed decreased membrane PKC β expression both with and without I/R injury. Although $TG^{SGLT1\text{-}DOWN}$ hearts exhibited no difference from wild-type hearts in PKC δ expression before ischaemia, there was decreased expression after reperfusion. Hence, the cardioprotective effect of SGLT1 knockdown may be related to initial decreased PKC β and phosphorylated p47phox expression leading to decreased ROS production, and later by inhibition of PKC δ during reperfusion.

Although activation of AMPK is generally beneficial in the cellular response to stresses such as ischaemia, our data suggest that one consequence, namely up-regulation of SGLT1, may in fact be deleterious. We and others[37] have established that, of seven SGLT isoforms (SGLT1 to 6 and sodium-myoinositol cotransporter-1 [SMIT1]), only SGLT1 and SMIT1 are expressed in human, mouse, and rat hearts. Therefore, development of specific antagonists for SGLT1 may attenuate the deleterious effects of SGLT1 in cardiac I/R, but leave other beneficial effects of AMPK intact. Of note, the $TG^{SGLT1\text{-}DOWN}$ mice used in this study exhibit approximately 80% knockdown of cardiomyocyte SGLT1 protein rather than complete knockout, reflecting a degree of inhibition likely similar to that which could be achieved pharmacologically. Several inhibitors of SGLT2, which is not expressed in the heart, have recently been approved for the treatment of diabetes. One inhibitor, empagliflozin, reduces cardiovascular death and heart failure in Type 2 diabetic patients,[44] by mechanisms that are distinct from its glucose-lowering effect.[45] Although these agents are much more selective for SGLT2 than SGLT1, it is intriguing to speculate whether the beneficial cardiovascular effects of empagliflozin are partly attributable to SGLT1 inhibition. Sotagliflozin, a new dual inhibitor of SGLT1 and SGLT2, is in clinical trials for diabetes (NCT02384941).

In summary, this is the first study to document that cardiac ischaemia-reperfusion activates a cascade of AMPK, ERK, SGLT1, EGFR, PKC, and Nox2 that leads to oxidative injury. Our preclinical data suggest that specific inhibition of SGLT1 may be salutary in attenuating ischaemic injury.

Supplementary material

Supplementary material is available at *Cardiovascular Research* online.

Conflict of interest: none declared.

Funding

This work was supported by the National Institutes of Health [R01 HL135000 to F.A. and U01 HL108642 to F.A.]; and the American Heart Association [15GRNT25650003 to F.A. and 16POST27770035 to Z.L.].

References

1. Wright EM, Loo DD, Hirayama BA. Biology of human sodium glucose transporters. *Physiol Rev* 2011;**91**:733–794.
2. Turk E, Zabel B, Mundlos S, Dyer J, Wright EM. Glucose/galactose malabsorption caused by a defect in the Na+/glucose cotransporter. *Nature* 1991;**350**:354–356.
3. Zhou L, Cryan EV, D'Andrea MR, Belkowski S, Conway BR, Demarest KT. Human cardiomyocytes express high level of Na+/glucose cotransporter 1 (SGLT1). *J Cell Biochem* 2003;**90**:339–346.
4. Banerjee SK, McGaffin KR, Pastor-Soler NM, Ahmad F. SGLT1 is a novel cardiac glucose transporter that is perturbed in disease states. *Cardiovasc Res* 2009;**84**:111–118.
5. Banerjee SK, Wang DW, Alzamora R, Huang XN, Pastor-Soler NM, Hallows KR, McGaffin KR, Ahmad F. SGLT1, a novel cardiac glucose transporter, mediates increased glucose uptake in PRKAG2 cardiomyopathy. *J Mol Cell Cardiol* 2010;**49**:683–692.
6. Arad M, Seidman CE, Seidman JG. AMP-activated protein kinase in the heart: role during health and disease. *Circ Res* 2007;**100**:474–488.
7. Nishino Y, Miura T, Miki T, Sakamoto J, Nakamura Y, Ikeda Y, Kobayashi H, Shimamoto K. Ischemic preconditioning activates AMPK in a PKC-dependent manner and induces GLUT4 up-regulation in the late phase of cardioprotection. *Cardiovasc Res* 2004;**61**:610–619.
8. Russell RR 3rd, Li J, Coven DL, Pypaert M, Zechner C, Palmeri M, Giordano FJ, Mu J, Birnbaum MJ, Young LH. AMP-activated protein kinase mediates ischemic glucose uptake and prevents postischemic cardiac dysfunction, apoptosis, and injury. *J Clin Invest* 2004;**114**:495–503.
9. Li J, Miller EJ, Ninomiya-Tsuji J, Russell RR 3rd, Young LH. AMP-activated protein kinase activates p38 mitogen-activated protein kinase by increasing recruitment of p38 MAPK to TAB1 in the ischemic heart. *Circ Res* 2005;**97**:872–879.
10. Gollob MH, Green MS, Tang AS, Gollob T, Karibe A, Ali Hassan AS, Ahmad F, Lozado R, Shah G, Fananapazir L, Bachinski LL, Roberts R, Hassan AS. Identification of a gene responsible for familial Wolff-Parkinson-White syndrome. *N Engl J Med* 2001;**344**:1823–1831.
11. Arad M, Benson DW, Perez-Atayde AR, McKenna WJ, Sparks EA, Kanter RJ, McGarry K, Seidman JG, Seidman CE. Constitutively active AMP kinase mutations cause glycogen storage disease mimicking hypertrophic cardiomyopathy. *J Clin Invest* 2002;**109**:357–362.
12. Arad M, Moskowitz IP, Patel VV, Ahmad F, Perez-Atayde AR, Sawyer DB, Walter M, Li GH, Burgon PG, Maguire CT, Stapleton D, Schmitt JP, Guo XX, Pizard A, Kupershmidt S, Roden DM, Berul CI, Seidman CE, Seidman JG. Transgenic mice overexpressing mutant PRKAG2 define the cause of Wolff-Parkinson-White syndrome in glycogen storage cardiomyopathy. *Circulation* 2003;**107**:2850–2856.
13. Ahmad F, Arad M, Musi N, He H, Wolf C, Branco D, Perez-Atayde AR, Stapleton D, Bali D, Xing Y, Tian R, Goodyear LJ, Berul CI, Ingwall JS, Seidman CE, Seidman JG. Increased alpha2 subunit-associated AMPK activity and *PRKAG2* cardiomyopathy. *Circulation* 2005;**112**:3140–3148.
14. Wolf CM, Arad M, Ahmad F, Sanbe A, Bernstein SA, Toka O, Konno T, Morley G, Robbins J, Seidman JG, Seidman CE, Berul CI. Reversibility of PRKAG2 glycogen-storage cardiomyopathy and electrophysiological manifestations. *Circulation* 2008;**117**:144–154.
15. Luptak I, Shen M, He H, Hirshman MF, Musi N, Goodyear LJ, Yan J, Wakimoto H, Morita H, Arad M, Seidman CE, Seidman JG, Ingwall JS, Balschi JA, Tian R. Aberrant activation of AMP-activated protein kinase remodels metabolic network in favor of cardiac glycogen storage. *J Clin Invest* 2007;**117**:1432–1439.
16. Ramratnam M, Sharma RK, D'Auria S, Lee SJ, Wang D, Huang XY, Ahmad F. Transgenic knockdown of cardiac sodium/glucose cotransporter 1 (SGLT1) attenuates PRKAG2 cardiomyopathy, whereas transgenic overexpression of cardiac SGLT1 causes pathologic hypertrophy and dysfunction in mice. *J Am Heart Assoc* 2014;**3**:
17. Claycomb WC, Lanson NA Jr, Stallworth BS, Egeland DB, Delcarpio JB, Bahinski A, Izzo NJ Jr. HL-1 cells: a cardiac muscle cell line that contracts and retains phenotypic characteristics of the adult cardiomyocyte. *Proc Natl Acad Sci U S A* 1998;**95**:2979–2984.
18. Zaha VG, Young LH. AMP-activated protein kinase regulation and biological actions in the heart. *Circ Res* 2012;**111**:800–814.
19. Martin MG, Wang J, Solorzano-Vargas RS, Lam JT, Turk E, Wright EM. Regulation of the human Na(+)-glucose cotransporter gene, SGLT1, by HNF-1 and Sp1. *Am J Physiol Gastrointest Liver Physiol* 2000;**278**:G591–G603.
20. Loflin P, Lever JE. HuR binds a cyclic nucleotide-dependent, stabilizing domain in the 3' untranslated region of Na(+)/glucose cotransporter (SGLT1) mRNA. *FEBS Lett* 2001;**509**:267–271.
21. Wang W, Fan J, Yang X, Furer-Galban S, Lopez de Silanes I, von Kobbe C, Guo J, Georas SN, Foufelle F, Hardie DG, Carling D, Gorospe M. AMP-activated kinase regulates cytoplasmic HuR. *Mol Cell Biol* 2002;**22**:3425–3436.
22. Yang X, Wang W, Fan J, Lal A, Yang D, Cheng H, Gorospe M. Prostaglandin A2-mediated stabilization of p21 mRNA through an ERK-dependent pathway requiring the RNA-binding protein HuR. *J Biol Chem* 2004;**279**:49298–49306.
23. Tan NY, Khachigian LM. Sp1 phosphorylation and its regulation of gene transcription. *Mol Cell Biol* 2009;**29**:2483–2488.
24. Lim S, Jin K, Friedman E. Mirk protein kinase is activated by MKK3 and functions as a transcriptional activator of HNF1alpha. *J Biol Chem* 2002;**277**:25040–25046.
25. Ishikawa Y, Eguchi T, Ishida H. Mechanism of beta-adrenergic agonist-induced transmural transport of glucose in rat small intestine. Regulation of phosphorylation of SGLT1 controls the function. *Biochim Biophys Acta* 1997;**1357**:306–318.

26. Ren J, Bollu LR, Su F, Gao G, Xu L, Huang WC, Hung MC, Weihua Z. EGFR-SGLT1 interaction does not respond to EGFR modulators, but inhibition of SGLT1 sensitizes prostate cancer cells to EGFR tyrosine kinase inhibitors. *Prostate* 2013;**73**: 1453–1461.
27. Qi D, Young LH. AMPK: energy sensor and survival mechanism in the ischemic heart. *Trends Endocrinol Metab* 2015;**26**:422–429.
28. Matsushima S, Tsutsui H, Sadoshima J. Physiological and pathological functions of NADPH oxidases during myocardial ischemia-reperfusion. *Trends Cardiovasc Med* 2014;**24**:202–205.
29. Wang J, Whiteman MW, Lian H, Wang G, Singh A, Huang D, Denmark T. A non-canonical MEK/ERK signaling pathway regulates autophagy via regulating Beclin 1. *J Biol Chem* 2009;**284**:21412–21424.
30. Castaneda-Sceppa C, Subramanian S, Castaneda F. Protein kinase C mediated intracellular signaling pathways are involved in the regulation of sodium-dependent glucose co-transporter SGLT1 activity. *J Cell Biochem* 2010;**109**:1109–1117.
31. Di Franco A, Cantini G, Tani A, Coppini R, Zecchi-Orlandini S, Raimondi L, Luconi M, Mannucci E. Sodium-dependent glucose transporters (SGLT) in human ischemic heart: a new potential pharmacological target. *Int J Cardiol* 2017;**243**:86–90.
32. Du J, Guan T, Zhang H, Xia Y, Liu F, Zhang Y. Inhibitory crosstalk between ERK and AMPK in the growth and proliferation of cardiac fibroblasts. *Biochem Biophys Res Commun* 2008;**368**:402–407.
33. Kim HS, Kim MJ, Kim EJ, Yang Y, Lee MS, Lim JS. Berberine-induced AMPK activation inhibits the metastatic potential of melanoma cells via reduction of ERK activity and COX-2 protein expression. *Biochem Pharmacol* 2012;**83**:385–394.
34. Gelinas R, Mailleux F, Dontaine J, Bultot L, Demeulder B, Ginion A, Daskalopoulos EP, Esfahani H, Dubois-Deruy E, Lauzier B, Gauthier C, Olson AK, Bouchard B, Des Rosiers C, Viollet B, Sakamoto K, Balligand JL, Vanoverschelde JL, Beauloye C, Horman S, Bertrand L. AMPK activation counteracts cardiac hypertrophy by reducing O-GlcNAcylation. *Nat Commun* 2018;**9**:374.
35. Hopf A-E, Andresen C, Kötter S, Isić M, Ulrich K, Sahin S, Bongardt S, Röll W, Drove F, Scheerer N, Vandekerckhove L, De Keulenaer GW, Hamdani N, Linke WA, Krüger M. Diabetes-induced cardiomyocyte passive stiffening is caused by impaired insulin-dependent titin modification and can be modulated by neuregulin-1. *Circ Res* 2018;**123**:342–355.
36. Kashiwagi Y, Nagoshi T, Yoshino T, Tanaka TD, Ito K, Harada T, Takahashi H, Ikegami M, Anzawa R, Yoshimura M. Expression of SGLT1 in human hearts and impairment of cardiac glucose uptake by phlorizin during ischemia-reperfusion injury in mice. *PLoS One* 2015;**10**:e0130605.
37. Kanwal A, Nizami HL, Mallapudi S, Putcha UK, Mohan GK, Banerjee SK. Inhibition of SGLT1 abrogates preconditioning-induced cardioprotection against ischemia-reperfusion injury. *Biochem Biophys Res Commun* 2016;**472**:392–398.
38. Sims MW, Winter J, Brennan S, Norman RI, Ng GA, Squire IB, Rainbow RD. PKC-mediated toxicity of elevated glucose concentration on cardiomyocyte function. *Am J Physiol Heart Circ Physiol* 2014;**307**:H587–H597.
39. Zhang L, Zhang Z, Guo H, Wang Y. Na+/K+-ATPase-mediated signal transduction and Na+/K+-ATPase regulation. *Fundam Clin Pharmacol* 2008;**22**:615–621.
40. Xia P, Kramer RM, King GL. Identification of the mechanism for the inhibition of Na+, K(+)-adenosine triphosphatase by hyperglycemia involving activation of protein kinase C and cytosolic phospholipase A2. *J Clin Invest* 1995;**96**:733–740.
41. Inagaki K, Hahn HS, Dorn GW, Mochly-Rosen D. Additive protection of the ischemic heart ex vivo by combined treatment with delta-protein kinase C inhibitor and epsilon-protein kinase C activator. *Circulation* 2003;**108**:869–875.
42. Liu Y, Jin J, Qiao S, Lei S, Liao S, Ge ZD, Li H, Wong GT, Irwin MG, Xia Z. Inhibition of PKCbeta2 overexpression ameliorates myocardial ischaemia/reperfusion injury in diabetic rats via restoring caveolin-3/Akt signaling. *Clin Sci* 2015;**129**:331–344.
43. Yang M, Stowe DF, Udoh KB, Heisner JS, Camara AK. Reversible blockade of complex I or inhibition of PKCbeta reduces activation and mitochondria translocation of p66Shc to preserve cardiac function after ischemia. *PLoS One* 2014;**9**:e113534.
44. Zinman B, Wanner C, Lachin JM, Fitchett D, Bluhmki E, Hantel S, Mattheus M, Devins T, Johansen OE, Woerle HJ, Broedl UC, Inzucchi SE; EMPA-REG OUTCOME Investigators. Empagliflozin, cardiovascular outcomes, and mortality in Type 2 diabetes. *N Engl J Med* 2015;**373**:2117–2128.
45. MacIsaac RJ, Jerums G, Ekinci EI. Cardio-renal protection with empagliflozin. *Ann Transl Med* 2016;**4**:409.